Structural optimization of atomic clusters using iterated dynamic lattice search: With application to silver clusters

Xiangjing Lai[a], Jin-Kao Hao[b,*], Zhaolu Guo[c], Quan Wen[d], Zhang-Hua Fu[e]

[a]*School of Business, Nanjing University of Information Science and Technology, Nanjing 210044, China*
[b]*LERIA, Université d'Angers, 2 Boulevard Lavoisier, 49045 Angers, France*
[c]*School of Science, JiangXi University of Science and Technology, Ganzhou 341000, China*
[d]*Institute of Advanced Technology, Nanjing University of Posts and Telecommunications, Nanjing 210023, China*
[e]*Institute of Robotics and Intelligent Manufacturing, The Chinese University of Hong Kong, Shenzhen 518172, China*

Computer Physics Communications, 2025, https://doi.org/10.1016/j.cpc.2025.109655

Abstract

Predicting the global minimum structures of atomic clusters has important practical implications in physics and chemistry. This is because the global minimum structures of their potential function theoretically correspond to their ground state structures, which determine some important physical and chemical properties of clusters. However, this prediction task is a very challenging global optimization problem due to the fact that the number of local minima on the potential energy surface of clusters increases exponentially with the cluster size. In this study, we propose an unbiased global optimization approach, called the iterated dynamic lattice search algorithm, to search for the global minimum structure of atomic clusters. Based on the iterated local search framework, the proposed algorithm employs the well-known monotonic basin-hopping method to improve the initial structures of clusters, a surface-based perturbation operator to randomly change the positions of selected surface atoms or central atom, a dynamic lattice search method to optimize the positions of surface atoms, and the Metropolis acceptance rule to accept the optimized new solutions. The performance of the algorithm is evaluated on the 300 widely studied silver clusters and experimental results show that the proposed algorithm is highly efficient compared to the existing algorithms. In particular, the proposed algorithm improves the best-known structures for 47 clusters and matches the best-known structures for the remaining clusters. Additional experiments

*Corresponding author
Email addresses: laixiangjing@gmail.com (Xiangjing Lai), jin-kao.hao@univ-angers.fr (Jin-Kao Hao), gzl@jxust.edu.cn (Zhaolu Guo), wenquan1412@163.com (Quan Wen), fuzhanghua@cuhk.edu.cn (Zhang-Hua Fu)

are performed to analyze the key components of the algorithm and the landscape of the potential energy surface of several representative clusters.

Keywords:
Structural Optimization, Atomic Clusters, Many-body Gupta Potential, dynamic Lattice Search, Global Optimization

---

1. Introduction

Finding the global minimum solution of a high-dimensional non-convex function is an important subject in various fields of science and research, such as determining the ground-state structures of clusters, crystals, and biomolecules (Ali et al., 2006; Wales and Scheraga, 1999). In physics and chemistry, predicting theoretically the ground-state structure of a cluster (i.e., the cluster optimization problem) by minimizing an empirical potential function with a global optimization method is an important issue, since the physical and chemical properties of cluster depend largely on its three-dimensional ground-state structure, which theoretically corresponds to the global minimum solution of the potential function (Wales and Scheraga, 1999).

However, determining the lowest-energy structure of atomic clusters is a very challenging global optimization task because the number of local minima of the potential function increases exponentially with the size of the cluster. For example, the number of local minima is more than 10^{10} on the potential energy surface (PES) of the 55-atom Lennard-Jones cluster (Wales and Scheraga, 1999). On the other hand, the main difficulty of optimization also comes from the competition between minima with similar energies but different structure types. That is, the highly competing local minima are separated by high barriers on the PES. For example, the 38-atom Lennard-Jones cluster has a double-funnel energy landscape in which each funnel corresponds to a type of structural motif, and the global minimum is located in a very narrow funnel with a face-centered cubic (FCC) motif on the PES (Doye et al., 1999).

Due to the practical importance and computational challenge of structural optimization of atomic clusters, a large number of approaches have been proposed in the literature to search for their global minimum structures. According to whether the algorithms use prior knowledge of the problem or information from putative global optimum structures, these approaches can be divided into two categories, i.e., the biased algorithms and the unbiased algorithms, where the biased algorithms employ the prior knowledge about the putative global minimum structures to improve the

efficiency of the algorithm. For example, based on the icosahedral lattice, which is constructed according to prior knowledge of the global minimum structure, Northby proposed a lattice-based search algorithm for determining the global minimum structure of Lennard-Jones clusters with $13 \leq N \leq 147$ (N is the number of atoms) (Northby, 1987), and Romero et al. presented a genetic algorithm combined with a stochastic search procedure for locating the global minimum structures of Lennard-Jones clusters in the range of $148 \leq N \leq 309$ (Romero et al., 1999). Based on the icosahedral and decahedral lattices, Xiang et al. proposed a greedy search method (GSM) for the Lennard-Jones clusters with $562 \leq N \leq 1000$ (Xiang et al., 2004). The advantage of these biased algorithms is that they can be efficiently applied to the large-scale clusters due to their high efficiency. However, these methods may miss the true global optimal solution because they restrict the search to the constructed lattice instead of the entire solution space.

In order to improve the search capability and overcome the shortcomings of biased algorithms, researchers from different fields have proposed a number of unbiased optimization algorithms for the structural optimization of atomic clusters in the literature. These algorithms belong to the category of stochastic optimization methods without assuming the structural features of the global minimum solution, and the initial configurations used by the algorithms are randomly generated. Moreover, the unbiased algorithms can be further divided into population-based evolutionary algorithms and trajectory-based iterative algorithms, according to the number of solutions involved in the search process. For the population-based algorithms, the most representative examples include the genetic algorithms (Hartke, 1995; Pullan, 1997, 2005, 2010; Zeiri, 1997; Shao et al., 2018), conformational space annealing algorithm (Lee et al., 2003), particle swarm optimization algorithms (Yan et al., 2017; Zhou et al., 2020), differential evolution algorithm (Fan et al., 2016), adaptive immune optimization algorithm (Cheng et al., 2004), and evolutionary programming approach (Iwamatsu, 2001). On the other hand, the most representative examples of trajectory-based iterative algorithms include the basin-hopping algorithm and its variants (Doye et al., 1999, 2004; Grosso et al., 2007; Locatelli and Schoen, 2002; Leary and Doye, 1999; Leary, 2000; Munro et al., 2002; Rondina and Da Silva, 2013; Wales and Doye, 1997), minima hopping algorithm (Goedecker, 2004), dynamic lattice search algorithm and its variants (Shao et al., 2004; Wu and Wu, 2014), heuristic algorithms with surface operator and interior operator (Takeuchi, 2006; Lai et al., 2011b), clustering methods (Bagattini et al., 2018) and Monte Carlo algorithm (Yu et al., 2019; Chen et al., 2022; Chen and Wang, 2021).

In this paper, we focus on the structural optimization of silver clusters described by the many-body Gupta potential (Gupta, 1981; Michaelian et al., 1999) for the following reasons. First, the structural optimization of silver clusters has been widely studied in the literature due to their important physical and chemical properties (Day et al., 2017; Duanmu and Truhlar, 2015; Grigoryan et al., 2013; Angulo and Noguez, 2008). Thus, they can serve as remarkable test systems for the structural optimization of atomic clusters. Second, the many-body Gupta potential is a popular potential function in the literature due to their strong ability to model the interactions among the atoms in the metal clusters such as Ni, Ag, Au, and Al clusters (Michaelian et al., 1999; Sdobnyakov et al., 2011; Keyampi et al., 2020) . Third, compared to the pair potential like the popular Lennard-Jones potential (Wales and Scheraga, 1999), the many-body Gupta potential is much more difficult to handle. Finally, it should be noted that the algorithm proposed in this study can also be adapted to optimize other atomic clusters with suitable modifications.

So far, a number of unbiased stochastic optimization algorithms have been proposed in the literature to search for the global optimal structures for silver clusters described by the Gupta potential. In 2005, Shao et al. proposed a random tunneling algorithm for the problem with up to $N = 80$ atoms (Shao et al., 2005). In 2006, Zhan et al. presented the first dynamic lattice search (DLS) algorithm and applied it to the clusters in the range of $61 \leq N \leq 120$ (Zhan et al., 2006). Their experimental results showed that their DLS algorithm significantly outperforms the previous algorithms and improves the best-known solutions for two clusters Ag_{79} and Ag_{80}. In 2007 and 2008, Yang et al. and Shao et al. respectively predicted the global optimal structures of silver clusters in the range of $13 \leq N \leq 160$ and some selected clusters in the range of $170 \leq N \leq 310$ by using the DLS algorithm as well as the DLS method with the constructed core (DLSc) (Yang et al., 2007; Shao et al., 2008). In 2011, through providing a more accurate definition for the energy of a single atom, Huang et al. designed two heuristic algorithms based on a modified dynamic lattice search method, and predicted systematically the global minimum structures of clusters with up to $N = 310$ atoms (Huang et al., 2011; Lai et al., 2011a). Their experimental results showed that the modified dynamic lattice search algorithm is very efficient compared to the previous dynamic lattice search methods and updated the best-known structures for a large number of clusters. In 2014, Wu et al. further optimized the clusters in the range of $N \leq 150$ by an adaptive immune optimization algorithm combined with the dynamic lattice search method and found an improved configuration for a small-scale cluster Ag_{61} (Wu and Wu, 2014). These studies imply that the dynamic lattice

search methods are the state-of-the-art approaches for the structure optimization of silver clusters described by the many-body Gupta potential.

From the literature review, we find that dynamic lattice search is a highly efficient approach and that its variants are the state-of-the-art algorithms for optimizing the silver clusters described by the Gupta potential. However, the existing algorithms still lack an efficient mechanism to systematically exploit the funnels on the potential energy surface (PES) of clusters, where a funnel on the PES corresponds to a category of structures and consists of a large number of local minima (see (Leary, 2000) for the detailed definition of the funnels on the PES). Therefore, it is very valuable to design a new algorithm able to systematically and deeply exploit each funnel on the PES.

The goal of this work is to design a highly efficient structure optimization algorithm by systematically exploiting the funnels on the PES of the atomic clusters. In particular, we focus on systematically optimizing the structures of silver clusters in the range of $N \leq 310$ due to the fact that the silver clusters in this size range have become a popular test system for evaluating the performance of cluster optimization algorithms, and a number of optimization algorithms have been tested on these clusters in the literature (Shao et al., 2005; Zhan et al., 2006; Yang et al., 2007; Shao et al., 2008; Huang et al., 2011; Lai et al., 2011a; Wu and Wu, 2014).

The main contributions of this work are summarized as follows.

1. We propose an unbiased structure optimization approach called the iterated dynamic lattice search (IDLS) algorithm for the metal clusters described by the many-body Gupta potential. The algorithm integrates a surface-based perturbation strategy, a highly efficient dynamic lattice search method, and the monotonic basin-hopping (MBH) method.
2. We systematically optimize the structures of 300 silver clusters from Ag_{11} to Ag_{310}, which are widely studied in the literature, by using the proposed algorithm. Experimental results show that the algorithm improves the best-known structures for 47 clusters and matches the best-known structures for the remaining 253 clusters.
3. The structural evolutions of the putative global optimum structures obtained are further analyzed for the silver clusters studied.

The remaining parts of paper are organized as follows. In Section 2, we describe in detail the proposed IDLS algorithm. In Section 3, the performance of IDLS algorithm is assessed by reporting the computational results on the silver clusters widely studied in the literature and making comparisons with the best-known results in the literature. Moreover, the evolution of putative

global minimum structures is further analyzed for the studied clusters. In Section 4, a key component of the algorithm is discussed to explain its influence on the performance of the algorithm, and the landscapes of the PES are analyzed for some representative clusters. In the last section, the present study is summarized and some research perspectives are provided for future research.

2. Iterated dynamic lattice search method

This section presents the proposed iterated dynamic lattice search (IDLS) algorithm for the metal clusters described by the many-body Gupta potential. The IDLS algorithm follows the general iterated local search framework (Lourenço et al., 2003; Stützle, 2006), which integrates a local search method, a perturbation operator, and an acceptance criterion for the new solutions. The algorithm uses the monotonic basin-hopping (MBH) method to improve the initial solution, a dynamic lattice search (DLS) method as the local search method, a surface-based perturbation operator to jump out of the local minimum traps, and the Metropolis acceptance rule to accept the improved solutions obtained by DLS. Before presenting the IDLS algorithm, we first describe the Gupta potential function, which is used to describe the interactions between atomic clusters.

2.1. Gupta potential

The many-body Gupta potential is based on the second moment approximation of the electron density of states in the tight-binding model and widely used to describe the interactions among the atoms of metal clusters (Michaelian et al., 1999). Given a cluster configuration $X = (r_1, r_2, \ldots, r_N)$ composed of N atoms in three-dimensional space R^3, where r_i denotes three-dimensional coordinates (x_i, y_i, z_i) of i-th atom, the Gupta potential energy $E(X)$ of X can be expressed as follows:

$$E(X) = \frac{U_N}{2} \sum_{i=1}^{N} V_i \tag{1}$$

$$V_i = A \sum_{j \neq i} exp[-p(\frac{r_{ij}}{r_0} - 1)] - \sqrt{\sum_{j \neq i} exp[-2q(\frac{r_{ij}}{r_0} - 1)]} \tag{2}$$

where r_{ij} represents the Euclidean distance between the i-th and j-th atoms, r_0 is the equilibrium nearest-neighbor distance in the bulk metal, and U_N is a function of the cluster size. Obviously, the Gupta potential contains a short-range repulsive pair potential term and an N-body attractive term, where the parameters p and q represent the repulsive interaction range and the attractive interaction

range, respectively, and the value of the parameter A was obtained by minimizing the bulk cohesive energy (Zhan et al., 2006).

In this study, we use the same parameter settings as in the previous studies for the Gupta potential, i.e., $A = 0.09944$, $p = 10.12$, $q = 3.37$, which was first obtained in (Michaelian et al., 1999) and then widely used in global optimization studies of silver clusters (Huang et al., 2011; Lai et al., 2011a; Shao et al., 2005; Wu and Wu, 2014; Zhan et al., 2006; Yang et al., 2007; Shao et al., 2008). In particular, for the parameters U_N and r_0, the reduced units are used, i.e., $U_N = 1.0$ and $r_0 = 1.0$, since their settings do not influence the cluster geometry structure. In other words, for a cluster configuration, if r_0 is set to a value other than 1 and the coordinates of all atoms in the cluster are simultaneously scaled by r_0, then all the distances r_{ij} $(i \neq j)$ between the atoms in the resulting configuration are also simultaneously scaled by r_0. As a result, both the geometry structure and the energy of the cluster will remain unchanged according to Eq. (2). Moreover, it should be noted that the equilibrium distance $r_0 = 2.8921$Å between the atoms in the silver clusters has been widely adopted in the literature (Alamanova et al., 2007; Wu et al., 2009).

Thus, for a cluster X with N atoms, the Gupta potential described by Eq. (1) is a non-convex function with $3N$ continuous variables, and the corresponding global optimization is a very challenging unconstrained optimization problem due to the fact the number of local minima increases exponentially with the cluster size on the PES of the cluster.

2.2. Main Framework of IDLS algorithm

As shown in the pseudo-code of Algorithm 1, the proposed IDLS algorithm is a three-phase heuristic algorithm, where X and X^* represent the current configuration and the best configuration found so far, respectively.

Starting from a randomly generated initial cluster configuration, the algorithm first uses the monotonic basin-hopping (MBH) method (Leary, 2000) to obtain a compact configuration, since the initial configuration is usually disordered and contains a number of holes (lines 2–14). At each iteration of MBH, the current configuration is perturbed, i.e., the coordinates of the atoms of the current solution are first shifted by a random displacement, i.e., $(x_i, y_i, z_i) \leftarrow (x_i, y_i, z_i) + \xi$ $(1 \leq i \leq N)$, where ξ is a uniform random vector in $[-0.8r_0, 0.8r_0]^3$, and then the obtained configuration is relaxed by the L-BFGS method (Liu and Nocedal, 1989). The resulting configuration is then accepted as the current solution if and only if the energy of the new cluster is lowered. The MBH

Algorithm 1: Main framework of the proposed IDLS algorithm

Function *IDLS()*
Input: Size of cluster (N), search depths β_1 and β_2, temperature T, parameters η_{min}, η_{max}, Δ_η
Output: The best solution found (X^*)

```
/* First Search Phase                                                    */
X ← InitialSolution(N)
X* ← L-BFGS(X)
NoImprove ← 0
while NoImprove ≤ β1 do
    X ← Random_Perturbation(X*)
    X ← L-BFGS(X)
    if E(X) < E(X*) then
        X* ← X, NoImprove ← 0
    else
        NoImprove ← NoImprove + 1
    end
end
/* Second Search Phase                                                   */
X ← X*, NoImprove ← 0, η ← η_min
while NoImprove ≤ β2 do
    X_o ← Surface_Perturbation(X, η)                  /* Algorithm 3 */
    X_o ← DLS(X_o)                                    /* Algorithm 2 */
    Δ_E = E(X_o) − E(X)
    if rand(0, 1) < e^(−Δ_E/T) then
        X ← X_o
    end
    if E(X_o) < E(X*) then
        X* ← X_o
        NoImprove ← 0
        η ← η_min
    else
        NoImprove ← NoImprove + 1
        η ← η + Δ_η
        if η > η_max then
            η ← η_min
        end
    end
end
/* Third Search Phase                                                    */
X_o ← Surface_Perturbation(X*, 1)                     /* Algorithm 3 */
X_o ← DLS(X_o)                                        /* Algorithm 2 */
if E(X_o) < E(X*) then
    X* ← X_o
end
```

method stops when the energy of the cluster cannot be lowered any further during β_1 successive perturbations, where β_1 is a parameter called the search depth of the MBH method.

Subsequently, based on the compact and ordered configuration from the first phase, the second phase of the algorithm aims to optimize the positions of the surface atoms of the cluster to further reduce its energy. This phase is the main search engine of the algorithm (lines 16–35) and can be considered as an iterated local search method, where a number of iterations are performed until the cluster energy cannot be improved during β_2 consecutive iterations, where β_2 is a parameter. At each iteration, the current solution X is randomly perturbed by a surface-based perturbation operator and then is locally improved by a dynamic lattice search (DLS) method which can be considered as a high-level local search method. After that, the solution X_o from the DLS method is accepted as the current solution according to the Metropolis criterion, i.e., the offspring solution is accepted as the current solution with a probability of $min\{1, e^{\frac{-\Delta_E}{T}}\}$, where $\Delta_E = E(X_o) - E(X)$ and T is the temperature parameter. Moreover, during the search process, the strength η of the perturbation operator is dynamically adjusted to achieve a good trade-off between search intensification and diversification (lines 27, 30–33). Thus, this search phase can also be considered as a large-step Monte Carlo algorithm (Martin, 1992) or an extended basin-hopping algorithm, where the DLS procedure acts as a strong local search method and the surface-based perturbation operator acts as a move operator.

The third phase consists of a surface-based perturbation operator and a DLS procedure (lines 37–41), whose goal is to create a central vacancy for the best configuration found so far. This stage is adopted based on the observation that for some large-scale clusters the putative optimal configuration has a central vacancy (Xiang et al., 2004; Chen et al., 2022). It should be noted that in this phase the surface-based perturbation operator only moves the highest-energy atom to the surface of the cluster, because the central atom has the highest energy for some icosahedral configurations (Xiang et al., 2004) and moving it to the surface of the cluster will create a central vacancy for the cluster and reduce significantly the energy of cluster. Finally, the best configuration X^* found is returned as the result of algorithm at the end of the search.

The following sections describe in detail the initial solution method, the dynamic lattice search method, and the surface-based perturbation operator.

2.3. Initial Solution

The initial configuration of the cluster is randomly generated in a spherical container with the center at the origin of the three-dimensional Cartesian coordinate system, and the radius R of the container is calculated as $r_0 \times (3N/4\pi)^{\frac{1}{3}}$, where N is the number of atoms and r_0 is the equilibrium distance between two atoms. To obtain an initial configuration of the cluster, all atoms are placed uniformly and randomly in the container and then the resulting configuration is relaxed by the L-BFGS method.

2.4. Dynamic Lattice Search Method

Algorithm 2: Dynamic Lattice Search (DLS) Method

Function *DLS()*
Input: A local minimum configuration X, parameter m
Output: The improved configuration X
do
  $X_0 \leftarrow X$
  $DL \leftarrow LatticeConstruction(X)$ /* Construct the dynamic lattice DL for the current configuration X */
  $\{X_1, X_2, \ldots, X_m\} \leftarrow LatticeSearch(X, DL)$ /* Search for m lowest-energy lattice minima based on DL with a discrete optimization method */
  for $i \leftarrow 1$ ***to*** m **do**
    $X_i \leftarrow$ L-BFGS(X_i) /* Relaxation of m lattice minima by a continuous optimization method L-BFGS */
  end
  $X_{min} \leftarrow arg\ min\{E(X_i) : i = 1, \ldots, m\}$
  if $E(X_{min}) < E(X)$ **then**
    $X \leftarrow X_{min}$ /* Update the current solution */
  end
while $E(X) < E(X_0)$

The dynamic lattice search (DLS) method (Shao et al., 2004) is a highly efficient iterative search algorithm and was originally proposed based on early optimization techniques of atomic clusters (Northby, 1987; Xue, 1994; Hartke, 1999) such as the directed mutation (Hartke, 1999). The current variant of DLS was developed in a previous study (Huang et al., 2011) by one of the present authors and was shown to be very efficient because of the new definition of the energy of

a single atom in the cluster. For the completeness of the description of our algorithm, we briefly introduce the DLS method from the point of view of continuous and discrete optimization, which provides several new insights and understandings.

The DLS method takes advantage of problem reduction techniques and discretization techniques of continuous solution space. At each iteration, the cluster optimization problem is first reduced into a smaller problem by fixing the positions of the low-energy atoms located usually in the interior of the cluster, and the fixed atoms constitute an interior core of the cluster and the remaining atoms are called active atoms, whose positions need to be optimized. Then, the resulting smaller continuous optimization problem is approximately converted into a discrete optimization problem by detecting the set of all possible stable positions on the surface of the cluster for an additional detecting atom, which is called the dynamic lattice (DL) of the current solution, and optimizing the positions of the active atoms over the constructed dynamic lattice. After that, the discrete optimization problem is solved by a discrete optimization method, and several high-quality local optimal solutions obtained are relaxed by a continuous local optimization method like L-BFGS (Liu and Nocedal, 1989). Thus, the DLS method can also be regarded as a dynamic continuous-discrete algorithm that alternately performs continuous and discrete optimizations until the energy of the cluster cannot be lowered.

The pseudo-code of the DLS method is given in Algorithm 2, where X denotes the current solution and the set $LM = \{X_1, X_2, \ldots, X_m\}$ denotes the set of lattice minimum solutions (see Section 2.4.2 for the definition). Starting from an input cluster configuration, the DLS method is performed iteratively until the energy can no longer be lowered. At each iteration, the construction of dynamic lattice (line 4), the lattice search procedure (the discrete optimization, line 5), and the local relaxations of lattice minimum solutions (the continuous optimization, lines 6-8) are in order performed to optimize the positions of the surface atoms. The main components of the DLS method are described in the following subsections.

2.4.1. Dynamic Lattice Construction

The lattice construction procedure aims to find all possible stable positions on the surface of the cluster for an additional atom. Specifically, these stable positions are determined via $2N$ random detections with an additional detecting atom. For each detection, the detecting atom is first randomly placed on the surface of the sphere with a radius of $0.7 \times R_{max}$ and a center located at

the cluster center, and then the position of the detecting atom is locally optimized by minimizing its potential energy, where R_{max} is the maximum distance from an atom in the cluster to the cluster center. The resulting position of the detecting atom is very stable for a single atom and called the lattice site. All the stable positions found by random detections and the positions occupied by N_{mov} highest-energy atoms in the cluster form a finite discrete set called the lattice DL, where N_{mov} is a parameter. Note that the lattice DL is dynamic and must be reconstructed at each iteration of the DLS method, hence it is called a dynamic lattice.

2.4.2. Lattice Search Procedure

When a dynamic lattice DL has been constructed for the current configuration, the DLS method employs a lattice search procedure to find several high-quality candidate solutions based on the constructed lattice. It can be found that the problem of selecting N_{mov} lattice sites from DL for the active atoms, such that the energy of the resulting configuration is minimized, is a discrete optimization problem. The size of the search space of this problem is very large and is equal to $C_{|DL|}^{N_{mov}} (= \frac{N_{move}!}{|DL|!(|DL|-N_{mov})!})$, where $|DL|$ and N_{mov} denote the size of dynamic lattice and the maximum number of active (or movable) atoms in the current iteration, respectively.

The lattice search procedure adopts a multi-start strategy combined with a greedy local search method, where N_{try} independent local search is performed to find several high-quality candidate solutions based on the lattice. For each local search, the initial cluster configuration is generated by randomly distributing N_{move} active atoms to distinct lattice sites of DL, while keeping the core of the cluster unchanged, and then is improved by a greedy local search method that iteratively moves the highest-energy active atom from its current position to the lowest-energy unoccupied lattice site until the energy of configuration cannot be lowered, where the energy $E(i)$ of a single atom i in the cluster X is defined as $E(i) = E(X) - E(X \setminus \{i\})$. The solution obtained by the greedy local search method is called a lattice minimum solution due to the fact that it is defined on the lattice DL. Finally, the first m different lowest-energy lattice minimum solutions obtained via N_{try} greedy searches are returned as the result of the lattice search procedure.

As indicated in Algorithm 2, these m lattice minimum solutions are relaxed in the continuous solution space by a continuous local optimization method (i.e., the L-BFGS method (Liu and Nocedal, 1989)) because there may be a small deviation between a lattice minimum solution and its local minimum solution in the continuous solution space. Thus, the search process of the algorithm

can be significantly accelerated because the time-consuming continuous optimization procedure is restricted to the lattice minimum solutions, instead of all lattice solutions.

2.5. *Surface-based Perturbation Operator*

Algorithm 3: Surface-based perturbation operator

1 **Function** *Surface_Perturbation()*
Input: A local minimum configuration X of cluster, perturbation strength η
Output: Perturbed configuration of cluster X_p
2 Calculate the potential energy for each atom in X
3 Sort the atoms in a descending order according to their energies E_i $(1 \leq i \leq N)$
4 Distribute randomly the first η highest-energy atoms on the surface of the sphere with a radius $0.7 \times R_{max}$, located at the cluster center

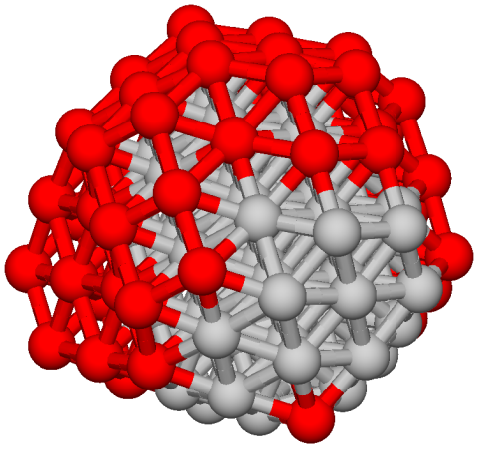

Figure 1: A local minimum configuration of Ag_{110}, where the first 55 highest-energy atoms are indicated in red.

Despite its strong search capability, the DLS method is still a local search approach and gets often stuck in local minima during the search process especially for large clusters. To jump out of local optimum traps reached by the DLS method, the IDLS algorithm employs a surface-based perturbation operator to perturb the current solution, whose pseudo-code is given in Algorithm 3.

The surface-based perturbation operator works as follows. Given a local minimum cluster configuration X, the atoms are first sorted in descending order of energy. Then, the first η highest-

energy atoms are redistributed by placing them randomly on the cluster surface, where η is a parameter called the perturbation strength, which is dynamically adjusted in the search process of IDLS. Specifically, these high-energy atoms are randomly distributed on the surface of a sphere with a radius of $0.7 \times R_{max}$, located at the cluster center, where R_{max} is the maximum distance from an atom in the cluster to the cluster center. Finally, the resulting configuration is locally improved by the L-BFGS method and returned as the result of the perturbation operator. This perturbation operator is designed based on the observation that the high-energy atoms are usually distributed on the cluster surface and it is very promising to further improve the energy of the whole cluster by optimizing their positions, where the energy $E(i)$ of atom i in the cluster X is calculated as $E(i) = E(X) - E(X \setminus \{i\})$. For an intuitive impression, we provide in Fig. 1 a graphical representation of a local minimum configuration. It can be seen that most of the high-energy atoms are distributed on the surface of the cluster, while the low-energy atoms are located in the interior of the cluster. In addition, the surface-based perturbation operator is also used to create the central vacancy for the cluster configuration, since the highest-energy atom is usually located at the center of cluster for large icosahedral configurations (Xiang et al., 2004; Chen et al., 2022). In this case, to create a central vacancy, the perturbation operator moves only the highest-energy atom to a random position on the surface of the cluster.

3. Computational Experiments and Assessments

In this section, we show computational results of the proposed algorithm and the new putative global optimal configurations found to evaluate the performance of the algorithm.

3.1. Parameter Setting and Experimental Protocol

Table 1: Setting of important parameters

Parameters	Section	Description	Values
β_1	2.2	search depth of MBH	50
β_2	2.2	search depth of the second phase of IDLS	20
T	2.2	temperature of IDLS	0.2
η_{min}	2.2	minimum strength of perturbation	15
η_{max}	2.2	maximum strength of perturbation	$N/4$
Δ_η	2.2	incremental value of perturbation	$N/20$
m	2.4	number of lattice minima in DLS	[5, 15]

The proposed IDLS algorithm has several parameters whose descriptions and settings are given in Table 1. The values of these parameters were empirically determined according to a preliminary

experiment and were adopted as the default parameter settings. In particular, the value of parameter m was set in the interval [5, 15] according to the size of the instances to be optimized.

The IDLS algorithm was written in C++[1] and compiled using the g++ compiler and all the computational experiments were carried out on a computer with an Intel E5-2670 processor (2.5 GHz and 2G RAM), running the Linux operating system. In addition, due to the stochastic behavior of the IDLS algorithm, the program was independently run 100 times with different random seeds for each instance in the range of $11 \leq N \leq 310$ to evaluate its average performance.

3.2. Computational Results and Assessment

We show the computational results of the IDLS algorithm on the clusters with $11 \leq N \leq 310$ to evaluate its performance.

3.2.1. New putative global optimal configurations

For the 300 clusters widely studied in the literature with $11 \leq N \leq 310$, the IDLS algorithm improves the best-known results for 47 clusters and matches the best-known solutions for the remaining clusters, where the best-known solutions are given in the well-known Cambridge landscape database (https://www-wales.ch.cam.ac.uk/CCD.html) for most clusters studied. The detailed computational results are summarized in Table 2 for the clusters for which the best-known configurations are improved by the algorithm, where the first two columns give the sizes of the clusters and the best-known potential energies in the literature, respectively. The detailed results of our algorithm are given in the remaining columns, including the best objective value (or energy) f_{best} over 100 independent runs, the average objective value f_{ave}, the worst objective value f_{worst}, the success rate SR to hit the best configuration, the standard deviation of the objective values obtained (σ), and the average computation times in seconds to reach the final solution ($time(s)$) for each run of the algorithm. To get an intuitive impression of the improved configurations of the clusters, we provide their geometric structures in Figs. 2 and 3.

Based on the fact that a number of global optimization algorithms have been tested on the silver clusters described by the many-body Gupta potential in the literature, one can observe from Table 2 that the proposed IDLS algorithm performs well and significantly outperforms the best-performing

[1]The source code of the IDLS algorithm will be publicly available at https://github.com/XiangjingLai/IDLS with the publication of the paper.

Table 2: Detailed computational results of the IDLS algorithm on the 47 clusters for which IDLS finds new best-known solutions, where the improved results are indicated in bold in terms of f_{best}.

		IDLS (This work)					
N	**BKR**	f_{best}	f_{avg}	f_{worst}	**SR**	σ	$time(s)$
59	-61.3969	**-61.4233**	-61.3864	-61.3433	4/100	1.27E-02	39
81	-85.4755	**-85.4757**	-85.4460	-85.2449	26/100	6.46E-02	101
143	-153.8282	**-153.8441**	-153.8173	-153.6362	17/100	4.36E-02	271
145	-156.1216	**-156.1500**	-156.0772	-155.8140	28/100	8.46E-02	300
146	-157.2794	**-157.3051**	-157.2357	-156.9265	19/100	9.63E-02	331
161	-173.7981	**-173.8057**	-173.6969	-173.5026	6/100	9.28E-02	524
165	-178.2196	**-178.2441**	-178.1510	-177.8710	1/100	1.04E-01	594
171	-184.8773	**-184.9341**	-184.8298	-184.5157	42/100	1.22E-01	596
172	-186.0265	**-186.0383**	-185.9557	-185.5584	48/100	1.30E-01	706
173	-187.1408	**-187.1961**	-187.0612	-186.5938	40/100	1.58E-01	666
177	-191.5945	**-191.6318**	-191.5470	-191.0749	57/100	1.32E-01	616
178	-192.7141	**-192.7412**	-192.6801	-192.2470	66/100	1.06E-01	788
181	-196.0920	**-196.1072**	-196.0078	-195.4945	37/100	1.42E-01	704
188	-203.8856	**-203.9006**	-203.8122	-203.2480	12/100	1.25E-01	792
190	-206.1572	**-206.1686**	-206.0510	-205.4797	2/100	1.49E-01	782
191	-207.3267	**-207.3418**	-207.2173	-206.6674	16/100	1.42E-01	1107
212	-230.6868	**-230.7031**	-230.5885	-230.1074	62/100	1.74E-01	1069
232	-252.9059	**-252.9247**	-252.8163	-252.2572	20/100	1.43E-01	1361
233	-254.0027	**-254.0824**	-253.9682	-253.5545	56/100	1.71E-01	1235
246	-268.5944	**-268.5968**	-268.4327	-267.7523	6/100	1.61E-01	1086
247	-269.7218	**-269.7303**	-269.5786	-269.2512	2/100	1.43E-01	1107
253	-276.4377	**-276.4466**	-276.2741	-276.0306	1/100	1.37E-01	1874
258	-282.0286	**-282.0865**	-281.8876	-281.5755	1/100	1.52E-01	1823
259	-283.2293	**-283.2447**	-283.0371	-282.6584	6/100	1.67E-01	1895
264	-288.7842	**-288.8403**	-288.5931	-288.1908	21/100	2.01E-01	2077
265	-289.9460	**-289.9617**	-289.7077	-288.7817	9/100	2.22E-01	2263
267	-292.1491	**-292.2126**	-291.9765	-291.6266	25/100	2.01E-01	2067
271	-296.6616	**-296.6772**	-296.4780	-295.9834	36/100	1.96E-01	2379
274	-299.9834	**-300.0426**	-299.8262	-299.2316	2/100	2.23E-01	2076
275	-301.1064	**-301.2008**	-300.9597	-300.5339	7/100	1.94E-01	1821
281	-307.9020	**-307.9176**	-307.6739	-307.1343	20/100	2.26E-01	2366
283	-310.0834	**-310.1677**	-309.9410	-309.2098	29/100	2.17E-01	2314
284	-311.2239	**-311.2341**	-311.0619	-310.6411	26/100	1.99E-01	2164
285	-312.3485	**-312.3598**	-312.1914	-311.7308	36/100	1.98E-01	1510
287	-314.6171	**-314.6327**	-314.4424	-313.9549	48/100	2.15E-01	2051
290	-317.9395	**-317.9981**	-317.7889	-317.3870	1/100	1.90E-01	2026
291	-319.0605	**-319.1562**	-318.9046	-318.3657	5/100	2.19E-01	2102
295	-323.5894	**-323.6016**	-323.3715	-322.7771	28/100	2.33E-01	2409
296	-324.6877	**-324.7521**	-324.5576	-323.9586	43/100	2.26E-01	2486
297	-325.8575	**-325.8729**	-325.6753	-325.1263	40/100	2.32E-01	2496
299	-328.0388	**-328.1226**	-327.9496	-327.3412	53/100	2.16E-01	2654
300	-329.0878	**-329.1896**	-329.0379	-328.2891	24/100	1.84E-01	2696
301	-330.3027	**-330.3155**	-330.1752	-329.6641	25/100	1.53E-01	2726
303	-332.5727	**-332.5884**	-332.4283	-331.8492	53/100	2.03E-01	2345
305	-334.7777	**-334.8400**	-334.6716	-333.8563	34/100	2.17E-01	3091
306	-335.9034	**-335.9378**	-335.7728	-335.1372	2/100	1.89E-01	2718
307	-337.0167	**-337.1113**	-336.9251	-336.1000	19/100	2.32E-01	2342

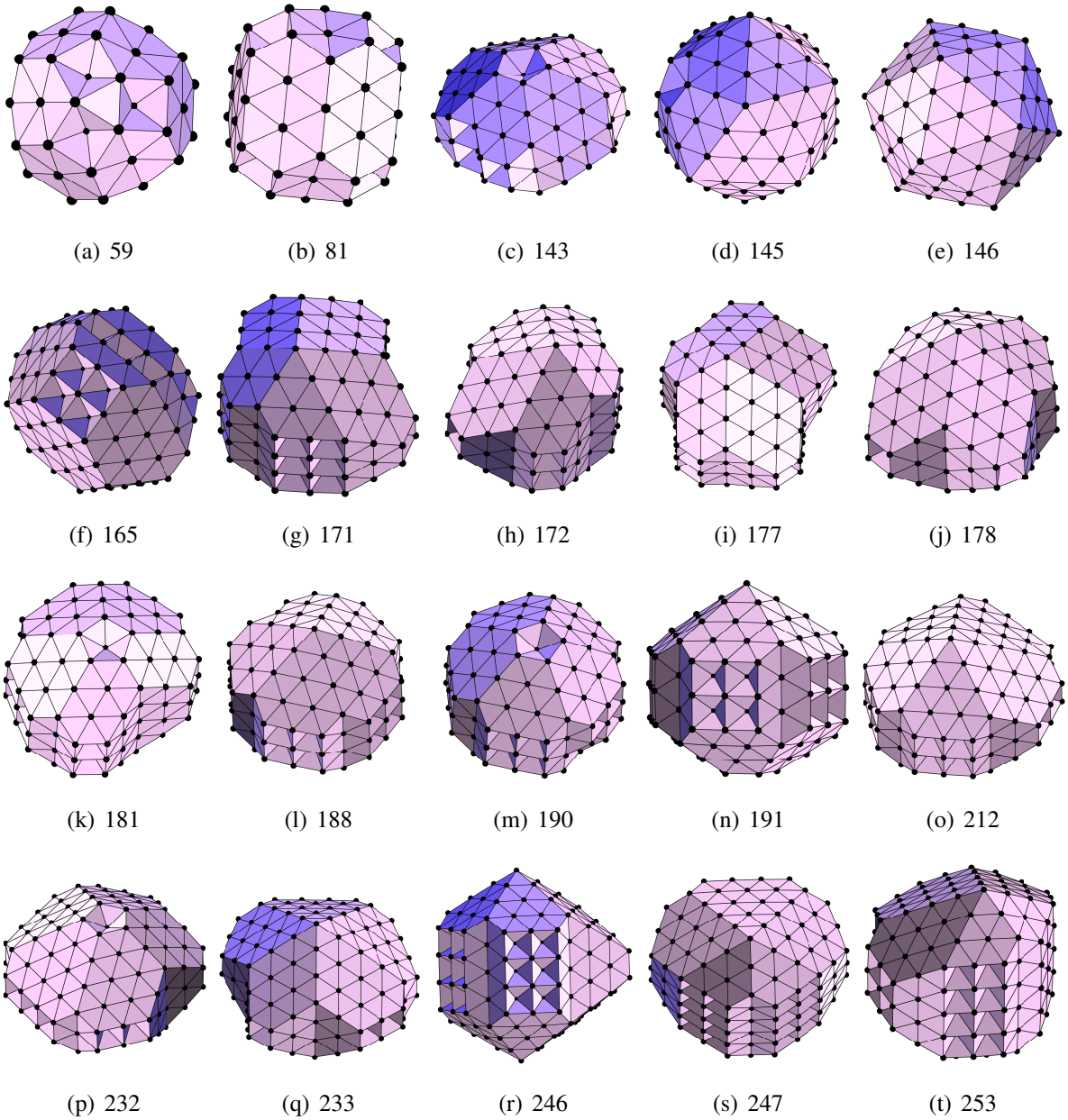

(a) 59 (b) 81 (c) 143 (d) 145 (e) 146

(f) 165 (g) 171 (h) 172 (i) 177 (j) 178

(k) 181 (l) 188 (m) 190 (n) 191 (o) 212

(p) 232 (q) 233 (r) 246 (s) 247 (t) 253

Figure 2: Improved configurations for several representative clusters with $N \leq 257$.

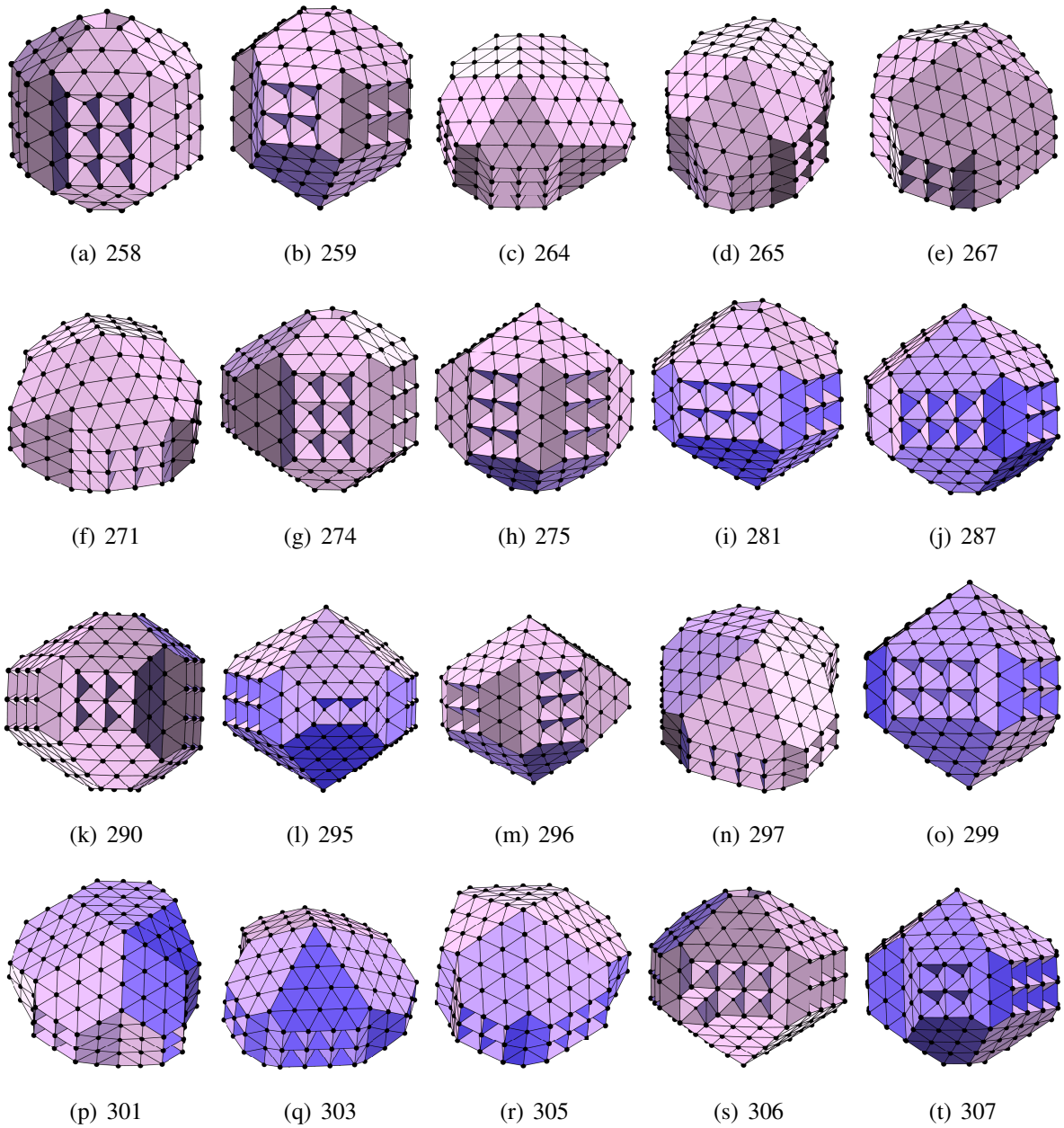

(a) 258 (b) 259 (c) 264 (d) 265 (e) 267

(f) 271 (g) 274 (h) 275 (i) 281 (j) 287

(k) 290 (l) 295 (m) 296 (n) 297 (o) 299

(p) 301 (q) 303 (r) 305 (s) 306 (t) 307

Figure 3: Improved configurations for several representative clusters with $258 \leq N \leq 310$.

algorithms in the literature by improving the best-known solution for a large number of clusters. In particular, for the small clusters with $N \leq 150$, which have been optimized by many global optimization algorithms, the IDLS algorithm improves the best-known solutions for five clusters, i.e., Ag_{59}, Ag_{81}, Ag_{143}, Ag_{145}, and Ag_{146}. As shown in Fig. 2, for the smallest cluster Ag_{59}, the new improved solution has a tetrahedral configuration, which is significantly different from the putative global optimal solution of other clusters. Moreover, the low success rate ($SR = 4/100$) of the algorithm on this cluster implies that the tetrahedral configuration corresponds to a very narrow funnel on the potential energy surface of the cluster and that it is difficult for the IDLS algorithm to locate the new improved solution. For Ag_{81}, the configuration of the improved solution belongs to the category of face-centered cube (FCC) structures, which is very difficult to locate by the previous optimization algorithms. In addition, it is worth noting that for Ag_{145} and Ag_{146}, the improved solutions have an icosahedral configuration with a central vacancy, i.e., the central atom of the configuration is missing due to its high energy. To the best of our knowledge, this is the first time to find that the putative global optimal configuration has a central vacancy for the small clusters with $N \leq 150$.

In terms of the robustness of the algorithm, one observes from Table 2 that the standard deviation of the objective values (i.e., the energies of the clusters) obtained for each cluster is very small, which means that the IDLS algorithm is very robust and is able to obtain the similar results in energy for all runs of the algorithm. Nevertheless, for several hard instances the success rate is very low, which means that there are several competing funnels on the PES of the cluster and the putative global minimum solution is located on a very narrow funnel. In terms of computational time, the performance of our algorithm is acceptable and the maximum time of a run is less than one hour for all instances.

In addition, Figs. 2 and 3 show that the vast majority of the new improved solutions have a decahedral configuration, including 11 truncated decahedral configurations. This result implies that the decahedral structures are still dominant configurations in the range of $N \leq 310$, which is consistent with the results of the previous studies (Yang et al., 2007; Shao et al., 2008; Huang et al., 2011; Lai et al., 2011a).

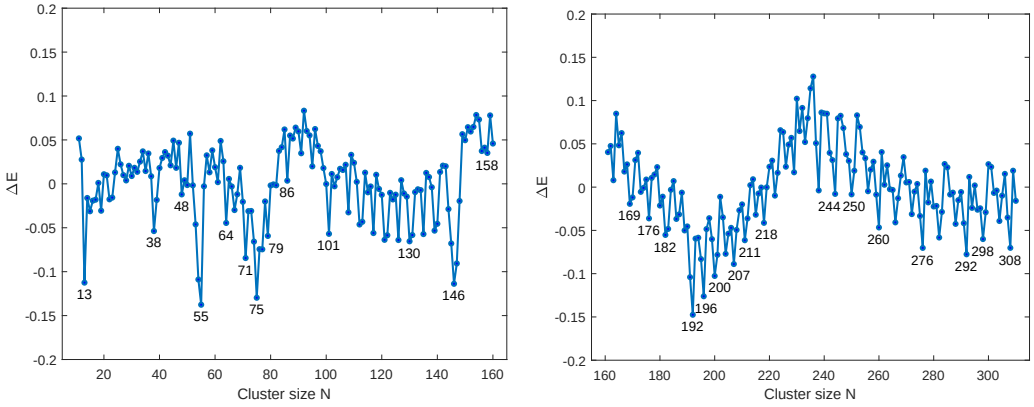

(a) $\Delta E(11 \leq N \leq 160)$

(b) $\Delta E(161 \leq N \leq 310)$

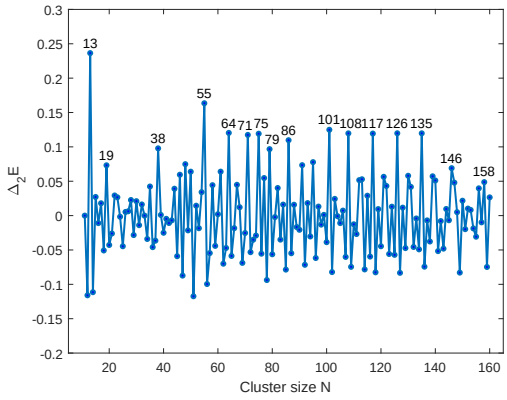

(c) $\Delta_2 E(11 \leq N \leq 160)$

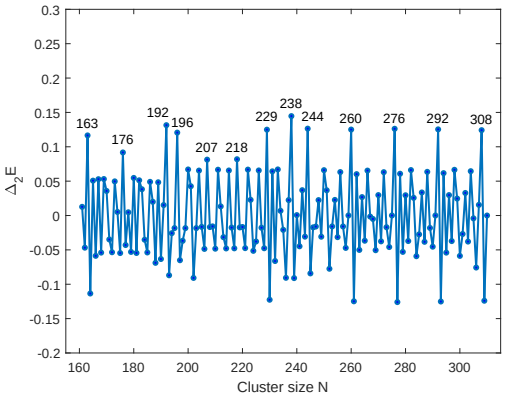

(d) $\Delta_2 E(161 \leq N \leq 310)$

Figure 4: Finite difference Δ_E and second finite difference $\Delta_2 E$ of the potential energies for the putative global minimum structures.

3.2.2. Magic numbers of clusters

To determine the magic numbers of Ag clusters, which corresponds to the cluster sizes for which the ground-state configurations are particularly stable compared to their neighboring sizes, we plot in Figure 4 the finite difference ΔE and the second finite difference $\Delta_2 E$ of the lowest energies found in this study as a function of the cluster size N, where a valley in ΔE and a peak $\Delta_2 E$ mean that the corresponding cluster has a particularly stable ground-state configuration and that the corresponding cluster size is a magic number. The finite difference ΔE of the potential energies is given in subfigures (a) and (b) of Figure 4, and the second finite difference $\Delta_2 E$ is given in subfigures (c) and (d). Specifically, the finite difference ΔE and the second finite difference $\Delta_2 E$ are respectively defined as follows.

$$\Delta E = E(N) - E_J(N) \tag{3}$$

$$\Delta_2 E = E(N+1) + E(N-1) + 2E(N) \tag{4}$$

where $E_J(N) = a + bN^{1/3} + cN^{2/3} + dN$ is a four-parameter fit of the lowest energies found in this work.

Figure 4 shows that most magic numbers are the same with those reported in the previous studies (Zhan et al., 2006; Huang et al., 2011; Yang et al., 2007), although the putative global optimum configurations are improved for 47 clusters in the present work. For instance, $N = 38$, 55, 75, 192 are still a magic number based on the current computational results, which means that the corresponding lowest-energy configurations are particularly stable compared to its neighboring sizes. Moreover, the new computational results indicate that $N = 146$ is a magic number missed in the previous studies and the new best configuration is an icosahedral one with a central vacancy. Note that the neighboring size $N = 147$ was wrongly identified as a magic number in the previous study (Huang et al., 2011).

3.2.3. Computation time and Success rate

To further investigate the performance of the IDLS algorithm, the average computation time (i.e., the average elapsed time from the start of the algorithm to the last update of the best solution found) and the success rate of the algorithm are systematically recorded and plotted as a function of the size of the cluster (N) in Fig. 5, where subfigures (a) and (b) give the average computation time and the success rate of our algorithm for each size, respectively.

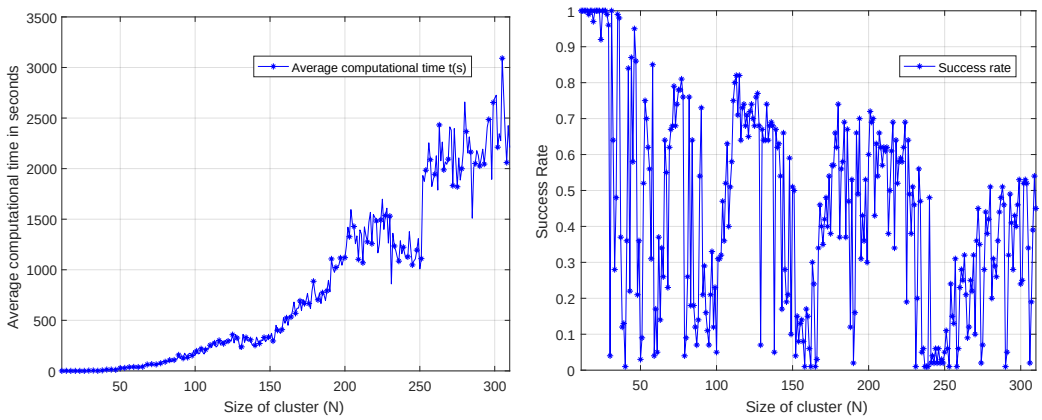

(a) Average computational time (b) Success rate

Figure 5: Average computation time of the IDLS algorithm for each run and success rate of the algorithm to hit the current best solution.

Fig. 5 shows that there is a general tendency that the computation time of the algorithm increases gradually as the size (N) of the cluster increases for the clusters in the range of $N \leq 200$. However, the computation time changes slightly for the clusters between $N = 200$ and 250, and then increases sharply at $N = 251$. For the larger clusters, the computation time fluctuates slightly as the size of cluster increases. The results of this experiment show that the larger clusters are generally more time-consuming to optimize compared to the smaller clusters for the proposed algorithm, and that the computation time varies slightly in several local ranges of cluster sizes. In addition, Fig. 5 shows that there exists an unexpected decrease in the average computational time for clusters within the size range $200 \leq N \leq 250$, and this implies that for these clusters the IDLS algorithm usually gets trapped in local (or global) minimum solutions located in a wide energy funnel on the PES of the cluster, thus leading to a search stagnation.

In terms of success rate, we observe that for most of the clusters, the success rate is greater than 0.3, which means that it is very likely that the global minimum solution has been found by the proposed algorithm for these clusters. However, there are still some clusters distributed in different size ranges whose success rates are smaller than 0.1, which means that these clusters are hard instances for the proposed algorithm. In particular, there are two size intervals (i.e., $[152, 166]$ and $[235, 253]$) where the success rate for most clusters is very low. This indicates that there are still a number of hard clusters for the proposed algorithm, although it significantly outperforms a number

of existing algorithms in terms of search capability.

4. Analysis and Discussions

We now analyze the effect of creating central vacancy on the searching ability of the algorithm, and provide a landscape analysis of the potential energy surface of the cluster for several representative instances.

4.1. Importance of creating central vacancy

Several studies show that for many large clusters (Chen et al., 2022; Xiang et al., 2004), the icosahedral configurations with central vacancy are the most stable structures. Thus, the third phase of the algorithm (see Algorithm 1), which aims to create a central vacancy for the configurations, is very key to increasing the robustness of the algorithm. To show the effectiveness of creating central vacancy, we perform an additional experiment on two representative clusters for which the putative optimal configuration is an icosahedral structure with a central vacancy, i.e., Ag_{145} and Ag_{146}. In this experiment, we first created a variant (denoted by IDLS-C) of the IDLS algorithm by disabling its third phase while keeping other components unchanged.

Then, we ran the IDLS and IDLS-C algorithms 100 times on each representative cluster, respectively. The experimental results of this experiment show that the success rates of the IDLS-C algorithm to hit the putative optimal configurations are 0/100 for two clusters, while the success rates of the IDLS algorithms are 28/100 and 19/100 respectively for the two representative clusters. This experiment shows that the third phase of the IDLS algorithm plays an important role in improving the robustness of the algorithm, and the creation of central vacancies is a necessary operation in finding the optimal configurations with a central vacancy. This may explain why all the previous algorithms failed to find the current best configurations for these two clusters.

4.2. Landscape Analysis of the PES for representative clusters

Many studies show that there exist a number of large funnels on the potential energy surface (PES) of clusters (Wales and Doye, 1997; Leary, 2000), where each large funnel corresponds to a category of structures, such as the tetrahedral structure (TE), the face-centered-cubic structure (FCC), the decahedral(DE) structure, and the icosahedral (IC) structure, where each large funnel consists of a large number of small funnels and each small funnel contains many local minima with

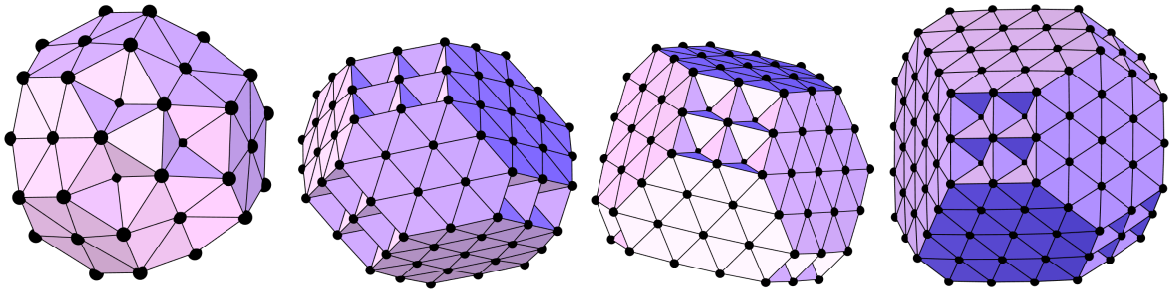

(a) N=59(SR=4/100) (b) N=158(SR=1/100) (c) N=162(SR=1/100) (d) N=231(SR=1/100)

Figure 6: Best configurations found for several hard instances.

very similar geometry structures. According to the computational results in Section 3.2, the putative optimal solutions found by the IDLS algorithm exhibit a decahedral structure for the majority of clusters studied. However, for several hard instances, the putative optimal solutions have a face-centered-cubic (FCC) or TE configuration. In Fig. 6, we give the putative optimal configurations of four representative hard clusters for which the success rate of our algorithm is no more than 4/100. We observe from the figure that these putative optimal solutions exhibit a FCC or TE configuration, which is different from the dominant decahedral structures. According to the potential energy surface theory (Wales and Doye, 1997; Cheng et al., 2005), the low success rate of the algorithm on these clusters means that the putative global optimal solution locates in a very narrow and deep funnel on the PES of the cluster and that it is very difficult for the IDLS algorithm to locate the global minimum configuration of these clusters.

To further analyze the landscape of the PES of clusters and investigate why some clusters are so difficult to optimize, we carried out another experiment based on six representative clusters, where an unbiased two-phase local search method is used to sample the configuration spaces of clusters. The two-phase local search method can be viewed as a high-level local search method and consists of the monotonic basin-hopping method and a dynamic lattice search method. In this experiment, the two-phase local search method was run 200 times for each cluster and the initial configuration of cluster was randomly sampled for each run of the two-phase local search method. For each cluster, 200 geometrical configurations obtained by the two-phase local search method are divided into five categories according to their structures, including the tetrahedral structure (TE), the face-centered-cubic structure (FCC), the decahedral(DE) structure, the icosahedral (IC)

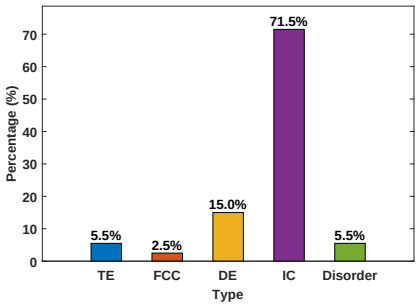

(a) N=59 (TE, SR=4/100)

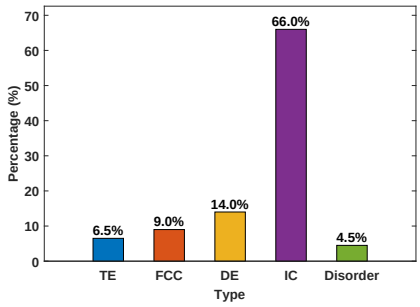

(b) N=158(FCC, SR=1/100)

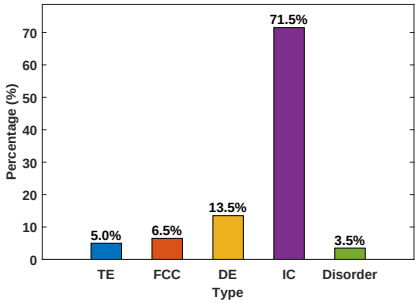

(c) N=162(FCC, SR=1/100)

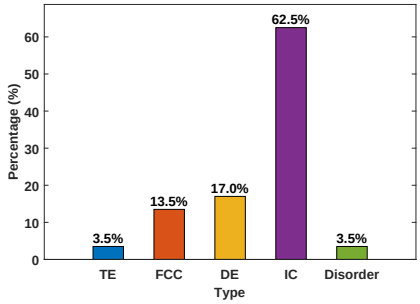

(d) N=165(FCC, SR=1/100)

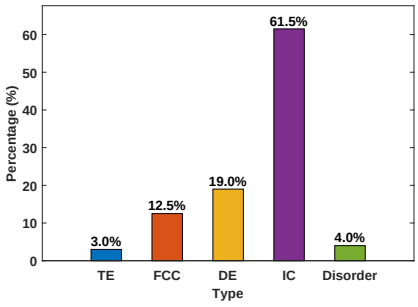

(e) N=178(DE, SR=66/100)

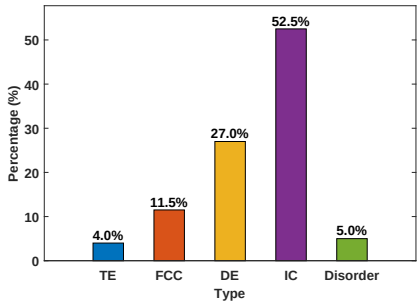

(f) N=231(FCC, SR=1/100)

Figure 7: The proportions of each category of structures over all 200 structures obtained by an unbiased two-phase local search method for six representative clusters.

structure, and the disordered structure. The proportions of each category of the structures over all obtained structures are summarized in Fig. 7 for each cluster, together with the putative optimal configuration of the cluster and the success rates of the IDLS algorithm, where a larger proportion means a wider funnel on the PES of the cluster for the corresponding category of structures.

We observe from Fig. 7 that for all tested clusters, the proportion of the IC structures is significantly larger than other categories of structures, which means that the funnel of the IC structures is very wide for these clusters and it is not very easy for an unbiased optimization algorithm to enter other categories of funnels. For the size $N = 59$, the putative global optimal solution has a TE structure, whereas the proportion of the TE structures is very low (=2.5%) on the PES of the cluster, which makes it very difficult for the unbiased algorithms to locate the putative global optimal solution. As a result, the success rate of IDLS is only 4/100. Similarly, for N =158, 162, 165 and 231, the putative global optimal solution has a FCC structure, whereas the proportion of the FCC structures is smaller than that of the IC and DE structures, which leads to a larger probability for the unbiased optimization algorithms to enter the IC and DE funnels of the PES of clusters than the FCC funnel and results in a very low success rate of the IDLS algorithm. On the contrary, for the size $N = 178$, the putative global optimal solution has a DE structure and the IDLS algorithm reaches a high success rate of 66/100. This phenomenon can be explained from the landscape of the PES of the cluster. For this cluster, the funnel of the putative global optimal solution on the PES has a large proportion of 19% that is larger than that of other funnels except for the IC funnel, which makes the IDLS algorithm enter the putative global optimal funnel with a high probability.

4.3. Discussion on the difference between theoretical and experimental results

The global minima of the cluster potential function theoretically correspond to the ground-state structures at the temperature of 0 K (Wales and Scheraga, 1999; Settem et al., 2023). To show whether our theoretical results are basically consistent with the experimental results, we made a rough comparison between the structures obtained by our IDLS algorithm and those synthesized by previous researchers in the laboratory. Specifically, using the electron microscopy, Giorgio and Urban (1988) studied the structures of small silver clusters in the experimental condition, and their study shows that the icosahedral configurations are more difficult to form than other structures for small clusters of about 1.0 nm (i.e., $N \leq 55$), which is consistent with the results obtained by the IDLS algorithm. In an electron diffraction study of clusters produced by inert-gas aggrega-

tion, Reinhard et al. (1997) found the icosahedral, decahedral and FCC configurations by mean of the high resolution electron microscopy for the silver clusters in the size range of $[3nm, 14nm]$, which is also consistent with the results of this work. Then, via the scanning transmission electron microscopy experiments, Loffreda et al. (2021) indicated that FCC is the predominant ordered structure for the silver clusters in the size range of $[302, 316]$, synthesized in vacuum. However, our results show that the decahedral configurations are the predominant structures for these silvers, which implies that the temperature may play a very important role for the cluster structures when two categories of structures are highly competing in the potential energy. In addition, the study of Vernieres et al. (2023) indicates that the air exposure will largely influence the structures of silver clusters in the synthesizing experiments.

These findings show that the structural motifs obtained by our IDLS algorithm are basically consistent with those synthesized in the laboratory especially for the small clusters. Nevertheless, for some large clusters, the structures obtained in this work differ from those synthesized in the laboratory due to the influences of the temperature or the air exposure. Thus, it is very important for the experimental researchers to consider the temperature as well as other conditions in synthesizing silver clusters in the laboratory.

5. Conclusions and Future Work

The structural optimization of metal clusters described by the many-body Gupta potential is an important and challenging global optimization problem with many important applications in physics and chemistry. In this study, we propose an unbiased global optimization algorithm, i.e., the iterated dynamic lattice search algorithm, for the structural optimization of atomic clusters described by the many-body Gupta potential. The proposed algorithm integrates mainly a surface-based perturbation operator, a dynamic lattice searching method, and a monotonic basin-hopping method. The algorithm was evaluated on 300 popular silver clusters with $11 \leq N \leq 310$ in the literature, showing an outstanding performance by reporting new best-known solutions for 47 clusters and matching the best-known solutions for the remaining clusters.

The experimental results indicate that for the putative global minimum structure, the decahedral configurations are still dominant for the silver clusters in the range of $N \leq 310$, as shown by the majority of the improved best solutions found by the proposed algorithm. Moreover, the landscape analysis on the PES of the clusters shows that the decahedral and icosahedral funnels are much

wider than other funnels for the studied clusters.

There are several research directions for future studies. First, the proposed algorithm can be adapted to other atomic clusters with different empirical potentials. Second, it is very interesting to design a hybrid evolutionary algorithm by integrating crossover and mutation operators and the dynamic lattice search method. Third, the proposed algorithm can be applied to the structural optimization of other metal clusters described by the many-body Gupta potential.

Acknowledgments. We are grateful to the reviewers for their valuable comments and suggestions, which helped us to improve the paper. We thank the Beijing Beilong Super Cloud Computing Co., Ltd for providing HPC resources that have contributed to the computational experiments reported in this work. This work was partially supported by the National Natural Science Foundation of China (Grant No. 61703213).

References

Alamanova, D., Grigoryan, V.G., Springborg, M., 2007. Theoretical study of the structure and energetics of silver clusters. The Journal of Physical Chemistry C 111, 12577–12587.

Ali, M., Smith, R., Hobday, S., 2006. The structure of atomic and molecular clusters, optimised using classical potentials. Computer Physics Communications 175, 451–464.

Angulo, A.M., Noguez, C., 2008. Atomic structure of small and intermediate-size silver nanoclusters. The Journal of Physical Chemistry A 112, 5834–5838.

Bagattini, F., Schoen, F., Tigli, L., 2018. Clustering methods for the optimization of atomic cluster structure. The Journal of Chemical Physics 148.

Chen, L., Liang, T., Wang, L., 2022. Growth pattern of large Morse clusters with medium-range potentials. The Journal of Physical Chemistry Letters 13, 9801–9808.

Chen, L., Wang, L., 2021. Unbiased fuzzy global optimization of Morse clusters with short-range potential for $N \leq 400$. Chinese Journal of Chemical Physics 34, 896–904.

Cheng, L., Cai, W., Shao, X., 2004. A connectivity table for cluster similarity checking in the evolutionary optimization method. Chemical Physics Letters 389, 309–314.

Cheng, L., Cai, W., Shao, X., 2005. Geometry optimization and conformational analysis of (C60)N clusters using a dynamic lattice-searching method. ChemPhysChem 6, 261–266.

Day, P.N., Pachter, R., Nguyen, K.A., 2017. A theoretical investigation of the structure and optical properties of a silver cluster in solid form and in solution. The Journal of Physical Chemistry A 121, 326–333.

Doye, J.P., Leary, R.H., Locatelli, M., Schoen, F., 2004. Global optimization of Morse clusters by potential energy transformations. INFORMS Journal on Computing 16, 371–379.

Doye, J.P., Miller, M.A., Wales, D.J., 1999. The double-funnel energy landscape of the 38-atom Lennard-Jones cluster. The Journal of Chemical Physics 110, 6896–6906.

Duanmu, K., Truhlar, D.G., 2015. Validation of methods for computational catalyst design: Geometries, structures, and energies of neutral and charged silver clusters. The Journal of Physical Chemistry C 119, 9617–9626.

Fan, T.E., Shao, G.F., Ji, Q.S., Zheng, J.W., Liu, T.d., Wen, Y.H., 2016. A multi-populations multi-strategies differential evolution algorithm for structural optimization of metal nanoclusters. Computer Physics Communications 208, 64–72.

Giorgio, S., Urban, J., 1988. Structure of 1 nm silver clusters. Journal of Physics F: Metal Physics 18, L147.

Goedecker, S., 2004. Minima hopping: An efficient search method for the global minimum of the potential energy surface of complex molecular systems. The Journal of Chemical Physics 120, 9911–9917.

Grigoryan, V., Springborg, M., Minassian, H., Melikyan, A., 2013. Optical properties of silver and copper clusters with up to 150 atoms. Computational and Theoretical Chemistry 1021, 197–205.

Grosso, A., Locatelli, M., Schoen, F., 2007. A population-based approach for hard global optimization problems based on dissimilarity measures. Mathematical Programming 110, 373–404.

Gupta, R.P., 1981. Lattice relaxation at a metal surface. Physical Review B 23, 6265.

Hartke, B., 1995. Global geometry optimization of clusters using a growth strategy optimized by a genetic algorithm. Chemical Physics Letters 240, 560–565.

Hartke, B., 1999. Global cluster geometry optimization by a phenotype algorithm with Niches: Location of elusive minima, and low-order scaling with cluster size. Journal of Computational Chemistry 20, 1752–1759.

Huang, W., Lai, X., Xu, R., 2011. Structural optimization of silver clusters from Ag141 to Ag310 using a modified dynamic lattice searching method with constructed core. Chemical Physics Letters 507, 199–202.

Iwamatsu, M., 2001. Applying evolutionary programming to structural optimization of atomic clusters. Computer Physics Communications 142, 214–218.

Keyampi, W., Tsasse, T., Nana, B., Zekeng, S., 2020. Global minimization of aluminum clusters using gupta potential. Chemical Physics Letters 754, 137635.

Lai, X., Huang, W., Xu, R., 2011a. Geometry optimization of atomic clusters using a heuristic method with dynamic lattice searching. The Journal of Physical Chemistry A 115, 5021–5026.

Lai, X., Xu, R., Huang, W., 2011b. Geometry optimization of bimetallic clusters using an efficient heuristic method. The Journal of Chemical Physics 135.

Leary, R.H., 2000. Global optimization on funneling landscapes. Journal of Global Optimization 18, 367–383.

Leary, R.H., Doye, J.P., 1999. Tetrahedral global minimum for the 98-atom Lennard-Jones cluster. Physical Review E 60, R6320.

Lee, J., Lee, I.H., Lee, J., 2003. Unbiased global optimization of Lennard-Jones clusters for $N \leq 201$ using the conformational space annealing method. Physical Review Letters 91, 080201.

Liu, D.C., Nocedal, J., 1989. On the limited memory BFGS method for large scale optimization. Mathematical Programming 45, 503–528.

Locatelli, M., Schoen, F., 2002. Fast global optimization of difficult Lennard-Jones clusters. Computational Optimization and Applications 21, 55–70.

Loffreda, D., Foster, D.M., Palmer, R.E., Tarrat, N., 2021. Importance of defective and nonsymmetric structures in silver nanoparticles. The Journal of Physical Chemistry Letters 12, 3705–3711.

Lourenço, H.R., Martin, O.C., Stützle, T., 2003. Iterated local search, in: Handbook of metaheuristics. Springer, pp. 320–353.

Martin, O., 1992. Large-step markov chains for the traveling salesman problem. Operations Research Letters 11, 219–224.

Michaelian, K., Rendón, N., Garzón, I., 1999. Structure and energetics of Ni, Ag, and Au nanoclusters. Physical Review B 60, 2000.

Munro, L.J., Tharrington, A., Jordan, K.D., 2002. Global optimization and finite temperature simulations of atomic clusters: Use of Xe_nAr_m clusters as test systems. Computer Physics Communications 145, 1–23.

Northby, J., 1987. Structure and binding of Lennard-Jones clusters: $13 \leq N \leq 147$. The Journal of Chemical Physics 87, 6166–6177.

Pullan, W., 1997. Genetic operators for the atomic cluster problem. Computer Physics Communications 107, 137–148.

Pullan, W., 2005. An unbiased population-based search for the geometry optimization of Lennard–Jones clusters: $2 \leq n \leq 372$. Journal of Computational Chemistry 26, 899–906.

Pullan, W., 2010. Unbiased geometry optimisation of Morse atomic clusters, in: IEEE Congress on Evolutionary Computation, IEEE. pp. 1–7.

Reinhard, D., Hall, B., Ugarte, D., Monot, R., 1997. Size-independent fcc-to-icosahedral structural transition in unsupported silver clusters: An electron diffraction study of clusters produced by inert-gas aggregation. Physical Review B 55, 7868.

Romero, D., Barrón, C., Gómez, S., 1999. The optimal geometry of Lennard-Jones clusters: 148–309. Computer Physics Communications 123, 87–96.

Rondina, G.G., Da Silva, J.L., 2013. Revised basin-hopping Monte Carlo algorithm for structure optimization of clusters and nanoparticles. Journal of Chemical Information and Modeling 53, 2282–2298.

Sdobnyakov, N.Y., Komarov, P., Sokolov, D., Samsonov, V., 2011. Study of the thermodynamic characteristics of gold nanoclusters using a gupta many-body potential. The Physics of Metals and Metallography 111, 13–20.

Settem, M., Roncaglia, C., Ferrando, R., Giacomello, A., 2023. Structural transformations in cu, ag, and au metal nanoclusters. The Journal of Chemical Physics 159.

Shao, G., Shangguan, Y., Tao, J., Zheng, J., Liu, T., Wen, Y., 2018. An improved genetic algorithm for structural optimization of Au-Ag bimetallic nanoparticles. Applied Soft Computing 73, 39–49.

Shao, X., Cheng, L., Cai, W., 2004. A dynamic lattice searching method for fast optimization of Lennard–Jones clusters. Journal of Computational Chemistry 25, 1693–1698.

Shao, X., Liu, X., Cai, W., 2005. Structural optimization of silver clusters up to 80 atoms with Gupta and Sutton-Chen potentials. Journal of Chemical Theory and Computation 1, 762–768.

Shao, X., Yang, X., Cai, W., 2008. Geometry optimization and structural distribution of silver clusters from Ag170 to Ag310. Chemical Physics Letters 460, 315–318.

Stützle, T., 2006. Iterated local search for the quadratic assignment problem. European Journal of Operational Research 174, 1519–1539.

Takeuchi, H., 2006. Clever and efficient method for searching optimal geometries of Lennard-Jones clusters. Journal of Chemical Information and Modeling 46, 2066–2070.

Vernieres, J., Tarrat, N., Lethbridge, S., Watchorn-Rokutan, E., Slater, T., Loffreda, D., Palmer, R.E., 2023. Influence of air exposure on structural isomers of silver nanoparticles. Communications Chemistry 6, 19.

Wales, D.J., Doye, J.P., 1997. Global optimization by basin-hopping and the lowest energy structures of Lennard-Jones clusters containing up to 110 atoms. The Journal of Physical Chemistry A 101, 5111–5116.

Wales, D.J., Scheraga, H.A., 1999. Global optimization of clusters, crystals, and biomolecules. Science 285, 1368–1372.

Wu, X., Cai, W., Shao, X., 2009. Optimization of bimetallic cu–au and ag–au clusters by using a modified adaptive immune optimization algorithm. Journal of Computational Chemistry 30, 1992–2000.

Wu, X., Wu, G., 2014. An adaptive immune optimization algorithm with dynamic lattice searching operation for fast optimization of atomic clusters. Chemical Physics 440, 94–98.

Xiang, Y., Cheng, L., Cai, W., Shao, X., 2004. Structural distribution of Lennard-Jones clusters containing 562 to 1000 atoms. The Journal of Physical Chemistry A 108, 9516–9520.

Xue, G., 1994. Improvement on the Northby algorithm for molecular conformation: Better solutions. Journal of Global Optimization 4, 425–440.

Yan, B., Zhao, Z., Zhou, Y., Yuan, W., Li, J., Wu, J., Cheng, D., 2017. A particle swarm optimization algorithm with random learning mechanism and Levy flight for optimization of atomic clusters. Computer Physics Communications 219, 79–86.

Yang, X., Cai, W., Shao, X., 2007. Structural variation of silver clusters from Ag13 to Ag160. The Journal of Physical Chemistry A 111, 5048–5056.

Yu, K., Wang, X., Chen, L., Wang, L., 2019. Unbiased fuzzy global optimization of Lennard-Jones clusters for $N \leq 1000$. The Journal of Chemical Physics 151.

Zeiri, Y., 1997. Study of the lowest energy structure of atomic clusters using a genetic algorithm. Computer Physics Communications 103, 28–42.

Zhan, H., Cheng, L., Cai, W., Shao, X., 2006. Structural optimization of silver clusters from Ag61 to Ag120 by dynamic lattice searching method. Chemical Physics Letters 422, 358–362.

Zhou, Y., Zhao, Z., Cheng, D., 2020. Cluster structure prediction via revised particle-swarm optimization algorithm. Computer Physics Communications 247, 106945.